

Acute entanglement and Photon/Phonons statistics in a balanced/unbalanced PT -symmetry systems

Muhammad Abid,¹ Areeda Ayoub,¹ and Javed Akram^{1,*}

¹*Department of Physics, COMSATS University Islamabad, Pakistan*

(Dated: November 3, 2022)

We study the significance of Photon/Phonons bunching and antibunching on the dynamics of the quantum entanglement in the presence of coupled PT -symmetry systems with balanced/unbalanced gain and loss. We suggest a hybrid electromechanical system to realize a strong and tunable coupling between a Coplanar-Waveguide (CPW) microwave cavity and a nanomechanical resonator (NAMR) via a superconducting Transmon qubit. The hybrid electromechanical system consists of a non-hermitian Hamiltonian with balanced/unbalanced gain and loss. The interplay between the quantum entanglement and the PT -symmetry systems is also thoroughly investigated. We frame a connection between Number operators, Photon/Phonons antibunching, and entanglement. It has been observed that the relative Photon/Phonons numbers play a key role in the quantum entanglement dynamics. Furthermore, we study that quantum entanglement can be characterized by defining a Photon/Phonons antibunching. The Photon/Phonons antibunching is strongly dependent on the initial squeezed state and the rate of balanced/unbalanced gain and loss of the system.

I. INTRODUCTION

Recently, the most promising idea pursued by the researchers is to combine two or more systems to form hybrid quantum systems, intending to harness the strengths and advantages of different physical systems in order to explore new physical phenomena and potentially give rise to novel quantum technologies [1–18]. They provide new tools and platforms to investigate deeper into unexplored quantum regimes. Among these systems, the nanomechanical resonators (NAMRs) embedded in qubits (including artificial atoms [1], spins [2], superconducting qubits [3, 4], and so on) are considered as a good candidate for exploring different quantum phenomena. For example, quantum entanglement [5, 6, 19], controllable coupling [7], hybrid quantum circuits [9], quantum squeezing [10, 11], quantum detection in nanomechanical systems [12], ground-state cooling [13–15] and phonon blockade [16] have already been proposed. Moreover, a controllable coupling between NAMR and Coplanar-Waveguide (CPW) microwave cavity has been realized through a qubit [17].

On the other hand, the PT -symmetry has been studied in different quantum systems [20–27]. A wide class of non-hermitian Hamiltonians respecting PT -symmetry exhibit entirely real spectrum of eigenvalues. The most interesting feature of such Hamiltonians is PT phase transition, in which the eigenvalues spectrum switches from being entirely real to being completely imaginary, which is marked by the presence of exceptional point (EP), where two or more eigenvalues and their corresponding eigenvectors coalesce and become degenerate [20]. Therefore, many interesting physical properties can also be studied with the PT symmetric device the dynamics of which is governed by an intrinsic quantum-mechanical law. For example, PT -symmetric Bose-Einstein condensate in a δ -function double-well po-

tential [21, 28], optomechanical devices as a phonon laser [22, 23], non-linear dynamics in cold atoms [25], and PT -symmetric circuit QED systems [26] have been proposed. Many intrinsic quantum properties have been studied with the help of PT devices such as decoherence dynamics [29], information retrieval and criticality [30], entanglement [31], and chiral population transfer [32, 33]. Moreover, due to the considerable progress in theories and experiments for the generation of mechanical gain and cavity loss [34, 35], more interesting properties have been studied. However, the true quantumness of PT system is still questionable because to preserve the proper commutation relation, quantum noises associated with the gain (amplifying) and loss (dampening) are often ignored, which shows a drastic difference than usual predictions [36–38].

Entanglement, being an inherent form of quantum correlation, has become an invaluable resource for quantum computing and quantum information processing. As it is well known that quantum entanglement is very fragile under the influence of environmental noises [39, 40]. Notably, due to the presence of quantum noises, the continuous variable (CV) entanglement generated in a system of two coupled waveguides is badly affected [41]. Therefore, experimentalists are mostly concerned to preserve the entanglement for a long time, as unavoidable interaction with an external environment is significantly detrimental to the generation of entanglement. A wide variety of decoherence entangled pairs such as photons [42], atoms [43], continuous Gaussian states [44], and spin chains [45] have been analyzed both experimentally and theoretically for the environment-induced sudden death of entanglement. The presence of quantum noise enables us to understand their effects in broken PT -symmetric systems more deeply.

In this article, we present a general framework for two paired quantum systems that adhere to PT -

symmetry. Relevant linear quantum systems shared balanced/unbalanced gain and loss with their neighbors. By defining unbalanced gain and loss, we try to understand the effects of quantum noises on entanglement. In this work, we describe the dynamical behavior of entanglement at exceptional points in the presence of balanced/unbalanced gain and loss. We study the effect of PT -symmetry exceptional point on the evolution of the number of photons and phonons with balanced/unbalanced gain and loss. We investigate the dynamics of a quantum correlation function in the different regimes across the exceptional points balanced/unbalanced gain and loss and try to build a relation between photon/phonon numbers and phase coherence. The rest of the paper is organized as follows. In Sec. II we present the description of the hybrid electromechanical system with the non-hermitian Hamiltonian. A hybrid electromechanical system to realize a strong and tunable coupling between a CPW microwave cavity and a NAMR via a superconducting Transmon qubit. The direct coupling between NAMR and CPW microwave cavities would be weak and uncontrollable as well due to their size mismatch. In Sec. III, we determine the effective Hamiltonian between the CPW microcavity and the NAMR by using the Fröhlich-Nakajima transformation. In Sec. IV, we illustrate the evolution of entanglement, photon/phonon numbers, and a kind of quantum correlation function in different regimes across the exceptional points. In the same section, we describe the effect of quantum noise on the dynamics of entanglement and the growth of photon/phonon numbers. Additionally, we also study the influence of squeezing on the dynamics of entanglement. In Sec. V, we discuss in detail how to do altering of the entanglement dynamics by changing the initial squeezing parameter for balanced and unbalanced scenarios. Finally, we conclude our findings in Sec. VI.

II. HAMILTONIAN OF THE HYBRID SYSTEM

We consider a hybrid electromechanical system, which consists of a superconducting CPW microwave cavity, a superconducting Transmon qubit, and a NAMR, as depicted in Fig. (1). The Hamiltonian of CPW microwave cavity can be expressed as $H_c = \hbar\omega_c c^\dagger c$, where $c(c^\dagger)$ denotes the bosonic annihilation (creation) operator of the cavity mode with resonant frequency $\omega_c = \sqrt{1/L_r C_r}$. Here, L_r and C_r , respectively, represent the total inductance and capacitance of the cavity. The Hamiltonian of the NAMR is defined as $H_m = \hbar\omega_m b^\dagger b$, with $b(b^\dagger)$ being the bosonic annihilation (creation) operator of the mechanical mode and ω_m is the resonant frequency of the NAMR. The Hamiltonian of superconducting Transmon qubit is given as $H_q = 4E_C(n - n_g)^2 - E_J \cos \phi$ [46], where n denotes the number of Cooper pairs, n_g describes the effective offset charge due to environmen-

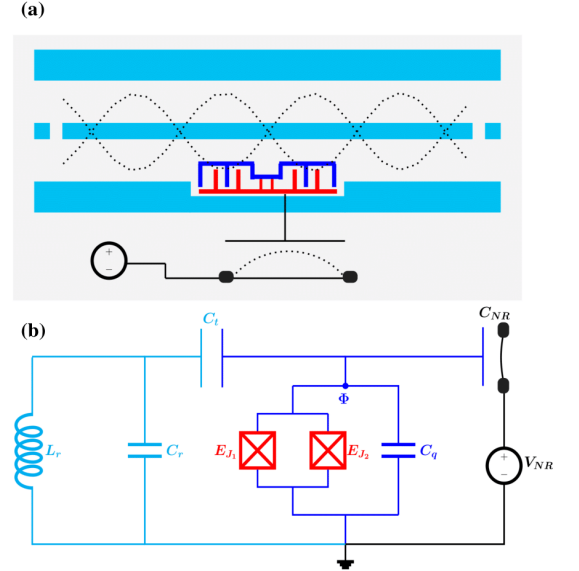


FIG. 1: (a) Schematic description of the hybrid electromechanical quantum system, which comprises a CPW microwave cavity, a superconducting qubit, and a NAMR. The coupling between the Transmon qubit and the NAMR can be achieved by applying external dc voltage in the NAMR. (b) Equivalent circuit of the hybrid quantum system.

tal sources and $E_C = e^2/2C_{eq}$ defines the charging energy of the capacitor, in which $C_{eq} = C_{NR}(x) + C_t + C_q$ is the total capacitance. $C_{NR}(x) = C_{NR}(1 - x/d)$ describes the capacitive coupling between the Transmon qubit and the NAMR as a function of resonator displacement x . Normally the length d is large as compared to the oscillation displacement x . C_t illustrates the coupling capacitance between the Transmon qubit and the CPW microwave cavity and C_q defines the total capacitance of the Transmon qubit. The effective Josephson coupling energy defines the Transmon qubit is given as $E_J = E_{J_1} + E_{J_2} = E_{J_0} \cos(\pi\Phi_{ext}/\Phi_0)$, where E_{J_0} is the maximum Josephson energy, Φ_{ext} is the externally applied magnetic flux, and Φ_0 is the superconducting magnetic flux quantum. In the rotating wave approximation, the effective Hamiltonian of the coupled system reads ($\hbar = 1$) [47]

$$H = \omega_c c^\dagger c + \omega_m b^\dagger b + \frac{\omega_q}{2} \sigma_z + g(c^\dagger \sigma_- + c \sigma_+) + \lambda(b^\dagger \sigma_- + b \sigma_+), \quad (1)$$

where ω_q and $\sigma_z = |e\rangle\langle e| - |g\rangle\langle g|$ denote, respectively, the transition frequency and the Pauli operator for the Transmon qubit. $\sigma_+ = |e\rangle\langle g|$ ($\sigma_- = |g\rangle\langle e|$) is the raising (lowering) operator, where $|e\rangle$ ($|g\rangle$) describes the excited (ground) state of the Transmon qubit. The coupling strength between the CPW microwave cavity and the Transmon qubit is defined as $g = -2V_{rms}^0 C_t / C_{eq} \hbar$, where $V_{rms}^0 = \sqrt{\hbar\omega_c / 2C_r}$ is the *rms* of vacuum volt-

age fluctuations of the CPW microwave cavity. $\lambda = x_{zpf}(4E_c V_{NR}/e\hbar)dC_{NR}/dx$ is the coupling strength between the NAMR and the qubit, where x_{zpf} represents the zero-point fluctuation of the NAMR oscillation displacement [48, 49], and V_{NR} is the applied external dc voltage to the NAMR. Thus, the physical properties of the hybrid quantum system can be adjusted by changing the external voltage, which modulate the coupling λ between the qubit and the NAMR.

III. EFFECTIVE COUPLING BETWEEN THE CPW MICROWAVE CAVITY AND THE NAMR

To decouple the Transmon qubit from hybrid quantum system, we use Fröhlich-Nakajima transformation [50] to Hamiltonian

$$H_{eff} = e^{-S} H e^S = H + [H, S] + [[H, S], S]/2 + \dots, \quad (2)$$

where

$$S = \frac{g}{\Delta_c} (c^\dagger \sigma_- + c \sigma_+) + \frac{\lambda}{\Delta_m} (b^\dagger \sigma_- + b \sigma_+). \quad (3)$$

We have considered the hybrid quantum system in dispersive regime where the detuning frequencies of the Transmon qubit from the CPW microwave cavity ($\Delta_c \equiv \omega_q - \omega_c > 0$) and NAMR ($\Delta_m \equiv \omega_q - \omega_{cm} > 0$), respectively, are much larger than the coupling strengths g and λ i.e., $g/\Delta_c \ll 1$ and $\lambda/\Delta_m \ll 1$. Since, both the coefficients g/Δ_c and λ/Δ_m are very small, the higher-order terms can be neglected and only the second-order term needs to be kept in Eq. (2). Therefore, the effective Hamiltonian can be rewritten as

$$H_{eff} \approx \omega_{c0} c^\dagger c + \omega_{m0} b^\dagger b - G(c^\dagger b + c b^\dagger), \quad (4)$$

where the effective microwave cavity frequency ω_{c0} , the effective NAMR frequency ω_{m0} , and the effective coupling strength G between the microwave cavity and the NAMR are defined as

$$\omega_{c0} = \omega_c - \frac{g^2}{\Delta_c}, \quad \omega_{m0} = \omega_m - \frac{\lambda^2}{\Delta_m}, \quad (5)$$

$$G = g\lambda \left(\frac{\Delta_c + \Delta_m}{2\Delta_c \Delta_m} \right).$$

While deriving Eq. (4), we have assumed that the Transmon qubit is at the ground state ($\sigma_+ \sigma_- = 0$). In this way, an effective coupling between the CPW microwave cavity and NAMR can be achieved by adiabatically eliminating the degrees of freedom of the qubit. From Eq. (5), we see that the frequencies of both the cavity mode and the mechanical mode are shifted due to their large detunings with the qubit, and the effective electromechanical coupling strength G depends upon the coupling strengths, g and λ , and the frequency detunings, Δ_c and Δ_m . By modulating the NAMR-qubit coupling strength λ with the external voltage, the effective electromechanical coupling G can be controlled.

IV. ENTANGLEMENT IN PT -SYMMETRIC ELECTROMECHANICAL SYSTEM

By considering the effect of the thermal environment, the quantum Heisenberg-Langevin equations for the system are written as

$$\dot{c} = -\left(i\omega_{c0} + \frac{\kappa}{2}\right)c + iGb + \sqrt{\kappa}c^{in}, \quad (6a)$$

$$\dot{b} = -\left(i\omega_{m0} - \frac{\gamma}{2}\right)b + iGc + \sqrt{\gamma}b^{in}, \quad (6b)$$

where κ defines the cavity loss and γ describes the mechanical gain. The vacuum input noise operators are defined as c^{in} and b^{in} , which satisfying following correlation functions:

$$\langle c^{in\dagger}(t)c^{in}(t') \rangle = 0, \quad (7a)$$

$$\langle c^{in}(t)c^{in\dagger}(t') \rangle = \delta(t - t'), \quad (7b)$$

$$\langle b^{in\dagger}(t)b^{in}(t') \rangle = n_{th}\delta(t - t'), \quad (7c)$$

$$\langle b^{in}(t)b^{in\dagger}(t') \rangle = (n_{th} + 1)\delta(t - t'), \quad (7d)$$

where $n_{th} = [\exp(\hbar\omega_{m0}/k_B T) - 1]^{-1}$ illustrates the mean thermal photon numbers of the mechanical resonator at temperature T and k_B describes the Boltzmann constant. Under the Markovian assumption, the noise operators c^{in} and b^{in} have zero mean values. Next, by introducing two slowly varying operators, $\tilde{c} = ce^{i\omega_{c0}t}$ and $\tilde{b} = be^{i\omega_{m0}t}$, Eq. (6) can be rewritten as

$$\dot{\tilde{c}} = -\frac{\kappa}{2}\tilde{c} + iG\tilde{b}e^{i(\omega_{c0}-\omega_{m0})t} + \sqrt{\kappa}\tilde{c}^{in}, \quad (8a)$$

$$\dot{\tilde{b}} = \frac{\gamma}{2}\tilde{b} + iG\tilde{c}e^{-i(\omega_{c0}-\omega_{m0})t} + \sqrt{\gamma}\tilde{b}^{in}. \quad (8b)$$

Here, we define two noise operators $\tilde{c}^{in} = ce^{i\omega_{c0}t}$ and $\tilde{b}^{in} = be^{i\omega_{m0}t}$, which possess the correlation functions as described in Eq. (7). We assume that the CPW microwave cavity is resonant with NAMR i.e., $\omega_{c0} = \omega_{m0}$ to obtain

$$\dot{\tilde{c}} = -\frac{\kappa}{2}\tilde{c} + iG\tilde{b} + \sqrt{\kappa}\tilde{c}^{in}, \quad (9a)$$

$$\dot{\tilde{b}} = \frac{\gamma}{2}\tilde{b} + iG\tilde{c} + \sqrt{\gamma}\tilde{b}^{in}. \quad (9b)$$

Next, we ignore quantum noises to recast Eq. (9) as $\dot{u}(t) = -i\tilde{H}u(t)$. Here, $u^T(t) = (q_1(t), p_1(t), q_2(t), p_2(t))$ is the state vector, which can be written in terms of dimensionless CV quadrature as $q_1 \equiv (c + c^\dagger)/\sqrt{2}$, $p_1 \equiv (c - c^\dagger)/i\sqrt{2}$, $q_2 \equiv (b + b^\dagger)/\sqrt{2}$ and $p_2 \equiv (b - b^\dagger)/i\sqrt{2}$. The non-Hermitian Hamiltonian of our system can be defined as

$$\tilde{H} = i \begin{pmatrix} \frac{\gamma}{2} & 0 & 0 & -G \\ 0 & \frac{\gamma}{2} & G & 0 \\ 0 & -G & -\frac{\kappa}{2} & 0 \\ G & 0 & 0 & -\frac{\kappa}{2} \end{pmatrix}. \quad (10)$$

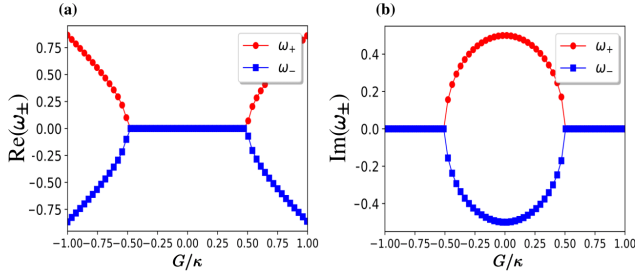


FIG. 2: For the case of balanced gain-loss i.e., $\gamma = \kappa$ (a) the real and (b) the imaginary parts the eigen frequencies ω_{\pm} are plotted as a function of dimensionless coupling strength G/κ .

It can be easily verified that the Hamiltonian \tilde{H} remains invariant under the simultaneous PT operation i.e., $[PT, \tilde{H}] = 0$. To study the PT phase transition, we first diagonalize the Hamiltonian and find the eigen frequencies of two supermodes

$$\omega_{\pm} = \frac{i(\gamma - \kappa)}{4} \pm \sqrt{G^2 - \left(\frac{\gamma + \kappa}{4}\right)^2} \quad (11)$$

where the real and imaginary parts correspond to the effective frequency and the dissipation in the system, respectively. From Eq. (11), we find that the eigenfrequencies ω_{\pm} of the two modes are highly dependent on the coupling strength G and there is a critical point $G_c = (\gamma + \kappa)/4$. Next, we consider the general situation where the mechanical gain and the cavity loss are defined with respect to each other i.e., $\gamma = s\kappa$, where s defines the ratio of gain and loss. By defining gain in terms of loss, we can rewrite critical coupling strength as $G_c = \kappa(s + 1)/4$.

A. Balanced Gain & Loss ($s = 1$)

In this subsection, we first study the dynamics of the hybrid electromechanical system for the case when the cavity loss and the mechanical gain are strictly balanced i.e., $\gamma = \kappa$ ($s = 1$). In this situation, the value of the critical coupling strength becomes $|G_c| = \kappa/2$. For the case of balanced gain and loss, the real and the imaginary parts of the eigenfrequencies ω_{\pm} are plotted as a function of dimensionless coupling strength G/κ , as shown in Fig. 2(a, b). It can be seen in Fig. 2(a, b), for $|G| > \kappa/2$ and $|G| < \kappa/2$, respectively, there exist two distinct phases: one that includes all the real eigenvalues named as the PT symmetric phase and the other which possesses purely imaginary eigenvalues named as broken PT symmetric phase. Both of these phases are separated by critical coupling strength $|G_c| = \kappa/2$, also known as an exceptional point (EP). Physically, the EP refers to the situation where the mechanical coupling rate G is balanced with the respective mechanical heating and cooling

rate. Then, for $|G| > \kappa/2$, we get a coherent exchange of energy between the CPW microwave cavity and the NAMR which corresponds to the PT symmetric phase and for $|G| < \kappa/2$ i.e., the coupling strength becomes weak enough to support the energy exchange, there is a localization of energy in the hybrid system which in turn leads to the broken PT symmetric phase.

Next, by taking quantum noises into account Eq. (9) can be written into more compact form as $\dot{u}(t) = Au(t) + n(t)$. Here, $u(t)$ is the same CV state vector, $A = -i\tilde{H}$ is the drift matrix and $n^T(t) = \sqrt{\kappa}X^{in}, \sqrt{\kappa}Y^{in}, \sqrt{\gamma}Q^{in}, \sqrt{\gamma}P^{in}$ is the matrix of corresponding noises. The input noise quadratures used in $n^T(t)$ are defined as: $X^{in} \equiv (\tilde{c}^{in} + \tilde{c}^{in\dagger})/\sqrt{2}$, $Y^{in} \equiv (\tilde{c}^{in} - \tilde{c}^{in\dagger})/i\sqrt{2}$, $Q^{in} \equiv (\tilde{b}^{in} + \tilde{b}^{in\dagger})/\sqrt{2}$, and $P^{in} \equiv (\tilde{b}^{in} - \tilde{b}^{in\dagger})/i\sqrt{2}$. The solution of this Langevin equation is given as $u(t) = e^{At}u(0) + \int_0^t ds e^{A(t-s)}n(s)$. The possible solutions of the system can be found for negative eigenvalues of A . It follows that only when the system remains in the PT symmetric phase, we can find such solutions.

We also observe that the system preserves its Gaussian properties due to the above-linearized dynamics and zero-mean Gaussian nature of the quantum noises. To completely describe the system, one can use the usual covariance matrix (CM) approach [51]. Let $W_{ij}(t)$ be the CM with each element defined as

$$W_{ij}(t) = \frac{\langle z | u_i(t)u_j(t) + u_j(t)u_i(t) | z \rangle}{2}. \quad (12)$$

Here, we consider a squeezed state as input state, i.e., $|z\rangle = e^{r(c^\dagger b^\dagger - cb)}|0, 0\rangle$, which is a two-mode squeezed vacuum state, with r being the squeezing parameter. For realization of such squeezed states in a hybrid system one may look into other striking proposals in Refs. [52–55]. The equation of motion as satisfied by the CM is given by:

$$\dot{W}(t) = AW(t) + W(t)A^T + Z. \quad (13)$$

Here, Z defines the matrix of noising correlation which is equal to $Z = [\frac{\gamma}{2} + \kappa(n_{th} + \frac{1}{2})]$ can be obtained by using the Markovian assumption and $(n_i(t)n_j(t) + n_j(t)n_i(t))/2 = \delta(t - t')Z_{ij}$. Eq. (13) is a first-order non-homogeneous differential equation that can be solved analytically and numerically by using proper initial conditions (Please see the appendix for an analytical solution). Here, our main concern is to investigate quantum entanglement. The formal solution of the Eq. (13) can be written as

$$W = \begin{pmatrix} W_A & W_{AB} \\ W_{AB}^T & W_B \end{pmatrix}, \quad (14)$$

where W_A , W_{AB} , W_B and W_{AB}^T are the 2×2 submatrices, respectively, corresponding to the local covariance matrices of the CPW microwave cavity and the

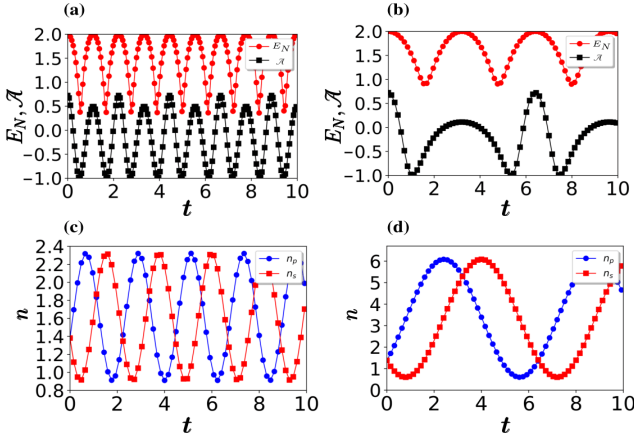


FIG. 3: For $s = 1$ (a) Entanglement evolution (line-circles) between the gain and loss resonators with antibunching (line-squares) for $G = 1.5$ (b) for $G = 0.7$. Dynamics of photon numbers (line circles) and phonons (line-squares) numbers for $G = 1.5$ (c) and $G = 0.7$ (d).

NAMR and the non-local correlation between them. One can calculate the so-called logarithmic negativity E_N to determine the degree of quantum entanglement, such as

$$E_N = \max[0, -\ln(2W^-)], \quad (15)$$

where $W^- \equiv \frac{1}{\sqrt{2}} \left[\sum(W) - \sqrt{\sum(W)^2 - 4 \det W} \right]^{\frac{1}{2}}$ is the smallest simplistic eigenvalue of the partial transpose of the W with $\sum(W) \equiv \det(W_A) + \det(W_B) - 2 \det(W_{AB})$. It is well established that the relative phase of the input fields plays important role in entanglement dynamics. Therefore, we also investigate nonclassicality feature and try to build a correlation between the entanglement and the antibunching. For the cavity and mechanical resonator modes c and b , respectively, the condition for inter-mode antibunching is defined as follows [56]

$$\mathcal{A}(b, c) = \frac{\langle b^\dagger c^\dagger b c \rangle - \langle b^\dagger b \rangle \langle c^\dagger c \rangle}{\langle c^\dagger c \rangle \langle b^\dagger b \rangle}. \quad (16)$$

Here, the first term on the right-hand side represents the simultaneous detection in the output of two coupled microwave cavities and the NAMR, while the second term defines the product of individual photon and phonons numbers. The time evolution of our system for the balanced gain-loss case is shown in Fig. (3). We have observed that when the system is in PT -symmetric phase the entanglement, antibunching, number of photons n_p , and number of phonons n_s oscillate periodically.

This oscillation could be ascribed by the nature of the eigenvalues $\pm \sqrt{G^2 - G_c^2}$ of A , as obtained for $G > G_c$. In Fig. 3(a), for $G = 1.5$, one can see that the entanglement oscillates rapidly with a smaller period and antibunching which is a non-classical feature oscillates briskly and

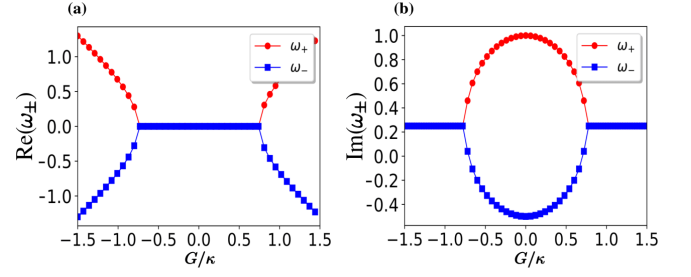


FIG. 4: For the case of unbalanced gain-loss i.e., $\gamma \neq \kappa$ (a) the real and (b) the imaginary parts the eigenfrequencies ω_{\pm} are plotted as a function of dimensionless coupling strength G/κ , here the value of $s = 2$.

have a positive value for maximum entanglement. However, when we approach near to the EP i.e., $G = 0.7$, we observe lesser oscillation with a smaller amplitude and longer period. So, in the close vicinity of the EP, the entanglement almost freezes out, which means that a longer period is required to complete one oscillation, as shown in Fig. 3(b). We investigate the acute entanglement happens only when the number of photons n_p and phonons n_s becomes equal during their oscillations as predicted in Fig. 3(c,d). One can observe that at $G = 1.5$, i.e., away from the EP, $n_p(t)$ and $n_s(t)$ oscillate very rapidly with very smaller time period. Whereas, in the close vicinity of the EP, n_p and n_s oscillate slowly with a longer period. The oscillatory behavior of the curves is attributed to the fact that the elements of the W matrix are sinusoidal. We also noticed that the entanglement becomes minimum when the difference of $n_p(t)$ and $n_s(t)$ becomes maximum and the entanglement becomes maximum when change between $n_p(t)$ and $n_s(t)$ becomes minimum. These results show that a direct connection between the number of photon/phonons, antibunching, and entanglement.

In this subsection, we consider the general situation when the mechanical gain and the cavity loss are not balanced, i.e., $s \neq 1$, with s being the gain-loss ratio. For the gain-loss ratio $s = 2$, i.e., $\gamma = 2\kappa$ means that in our system mechanical gain is larger as compared to the cavity-loss. In Fig. 4(a, b), we plot the eigenfrequencies of the system, which looks identical to Fig. (2), however, the imaginary part of the eigenfrequency is shifted at 0.25 from zero, this shifted eigenfrequency responsible for the gain in the overall system. In another way, we can say that in an unbalanced gain-loss case eigenfrequencies ω_{\pm} are not purely real and the system will always be in broken PT symmetric phase, as shown in Fig. 4(a, b). As compared to the balanced gain-loss rate, we observe that with the larger gain, the critical point G_c has been shifted to the right and a stronger coupling strength G is required in this situation to enter into a so-called exceptional point. Moreover, we also study the dynamics of our

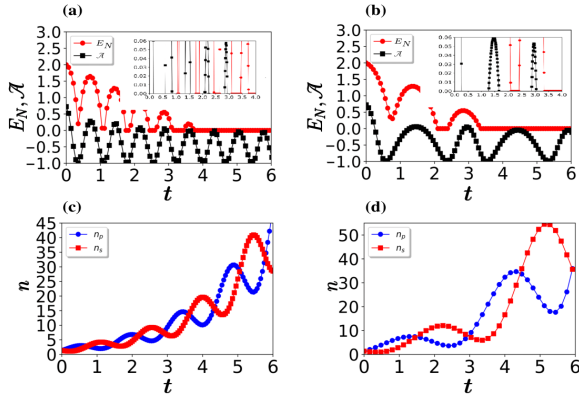


FIG. 5: For $s = 2$ (a) Entanglement (line-circles) and antibunching (line-squares) evolution for the hybrid system for $G = 2.3$ (b) for $G = 1.3$. In (a) and (b), inlet is plotted to emphasize the positive values of antibunching. Dynamics of photon numbers (line-circles) and phonons numbers (line-squares) for $G = 2.3$ (c) and $G = 1.3$ (d).

system for the unbalanced gain-loss case. In Fig. 5(a), we show the entanglement evolution for $s = 2$. One can see that for unbalanced gain-loss cases, oscillations decrease with time and eventually decays to zero a typical entanglement sudden death-like behavior, which means that unbalanced gain-loss rate adds noise into our system due to which entanglement ceases to oscillate and eventually dies out. However, a notable feature is the delayed entanglement death which can be achieved by pushing the system away from the EP i.e., $G = 0.75$, as predicted in Fig. 5(b). We also investigate the antibunching phenomenon for this special scenario which shows a positive magnitude for the maximum entanglement. We note that the non-classical feature i.e., antibunching phenomenon can not be measured for weak entanglement. In the sub-Fig. 5(a,b) we plot the zoom out of the antibunching phenomenon, to show the positive magnitude of the antibunching phenomena. In this case, we also note that when the difference of $n_p(t)$ and $n_s(t)$ becomes maximum, the entanglement grows and vice versa. We realize that for the unbalanced gain-loss case both n_p and n_s grow together, waning the distinction between gain and loss hybrid system. Since there is more gain in the system, therefore the n_p and n_s increase and it is due to external pumping into the system. We also find out that the number of photons and phonons grows exponentially which leads to a classical system therefore the entanglement dies out even though the difference between $n_p(t)$ and $n_s(t)$ becomes zero.

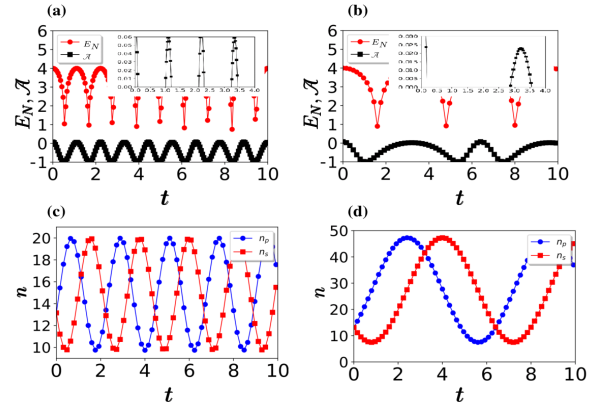


FIG. 6: Entanglement (line-circles) and antibunching (line-squares) evolution of hybrid electromechanical system for $G = 1.5$ (a) and for $G = 0.7$ (b) for $s = 1$ and $r = 2$. In (a) and (b), inlet is plotted to emphasize the positive values of antibunching. Dynamics of number of photons (line-circles) and phonons (line-squares) for $G = 1.5$ (c) and $G = 0.7$ (d).

V. ALTERING THE ENTANGLEMENT BY SQUEEZING PARAMETER

In this section, we investigate the effect of squeezing parameter r on quantum engagement dynamics for balanced and unbalanced hybrid PT electromechanical systems. For the **balanced** $s = 1$ cavity loss and mechanical gain, and for the squeezing parameter $r = 2$, the logarithmic negativity oscillates between $[0, 4]$ as shown in Fig. 6(a-b). The initial average number of photons is increased ten times as predicted in Fig. 6(c-d), in comparison to the scenario when squeezing parameter $r = 1$ as represented in Fig. 2(c-d). We note that the change in the squeezing parameter has no big impact on the oscillation of entanglement, antibunching, and the number of photon/phonons other than their magnitude as depicted in Fig. 2(a-d) and 6(a-d). For the **unbalanced** $s = 2$ cavity loss and mechanical gain, and for the squeezing parameter $r = 2$, we note that the so-called sudden death of the entanglement time delay is increased predicted in Fig. 7(a-b) as compared to the Fig. 5(a-b). It means that the strong squeezing prolongs the sudden death of the entanglement and reduces the influence of quantum noise on entanglement. The strong squeezing also increases the number of photons and phonons as depicted in Fig. 7(c-d). For the weak squeezing $r = 0.1$, we note that the dynamics of the entanglement oscillate periodically. Additionally, we also find out that the amplitude of the entanglement dynamics increases near the exceptional point for the balanced gain and loss system as shown in Fig. 8(a). For the unbalanced gain and loss system, we note that the significant delay in entanglement sudden death can be realized by pushing the electromechanical quantum system towards an exceptional point

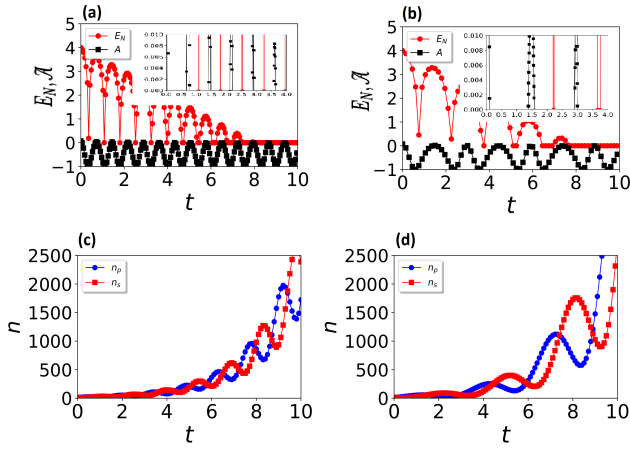


FIG. 7: Entanglement (line-circles) and antibunching (line-squares) evolution of hybrid electromechanical system for $G = 2.3$ (a) and for $G = 1.3$ (b) for $s = 2$ and $r = 2$. In (a) and (b), inset is plotted to emphasize the positive values of antibunching. Dynamics of number of photons (line-circles) and phonons (line-squares) for $G = 2.3$ (c) and $G = 1.3$ (d).

as illustrated in Fig. 8(b).

VI. CONCLUSION AND SUMMARY

In this study, we studied a gain-loss hybrid electromechanical system and emphasized the conditions necessary for exhibiting parity-time (PT) invariance. To realize a strong and tunable coupling between a Coplanar-Waveguide (CPW) microwave cavity and a nanomechanical resonator (NAMR) we purposed coupling of this hybrid system through a superconducting Transmon qubit. We examine the hybrid electromechanical system as a non-hermitian Hamiltonian with balanced/unbalanced gain and loss. The gain in our system is introduced in the NAMR and the loss of the system is defined for the CPW when gain and loss are balanced in the hybrid system the energy spectrum gets a real spectrum after the exceptional point. However, when the gain and loss do not equal, then the energy spectrum has some constant imaginary value that defines the gain in the system. With this setting, we examined the entanglement, antibunching, average photon, and phonon number with the initial squeezed state. We found out that the time of entanglement sudden death can be delayed near the exceptional points.

We also noticed that the entanglement gets maximum when the difference between the photons and phonons becomes minimum. We further examined a non-classical feature like antibunching for different balanced and unbalanced scenarios. We found out that the entanglement gets maximum when the antibunching gets positive. Later, we showed that for unbalanced gain-

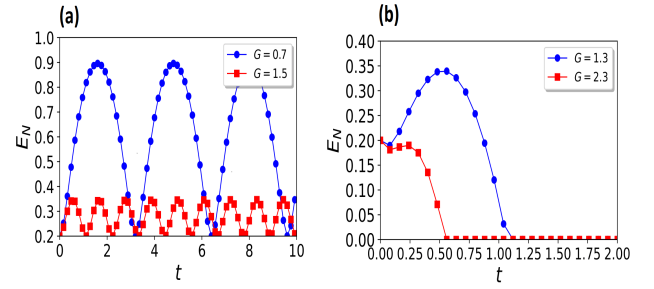


FIG. 8: Entanglement evolution of hybrid electromechanical system for balanced $s = 1$ (a) and for unbalance $s = 2$ (b) system, when the squeezing parameter is defined as $r = 0.1$

loss cases, oscillations decrease with time and eventually decay to zero a typical entanglement sudden death-like behavior, which means that an unbalanced gain-loss rate adds noise into our system due to which entanglement ceases to oscillate and eventually dies out. In the end, we investigated the dependence of the entanglement dynamics on the initial squeezing parameter, we analyzed that the initial squeezing parameter is not affecting the dynamics of the entanglement for the balanced gain and loss scenario. However, for unbalanced gain and loss, the sudden death of entanglement can be delayed by increasing the initial squeezing parameter. For the weak initial squeezing parameter, the significant delay in entanglement sudden death can be achieved even in a noisy environment. The present study helps to understand the role of PT -symmetry in the dynamics of the entanglement and in facilitating the preservation of the entanglement for a longer period. With this study, we build a relation between entanglement, antibunching, and the photons and phonons numbers in the physical systems, which are very much relevant in the field of quantum optics and quantum information processing.

Finally, we give a brief description of the experimental prospect of our proposed system. In our system, an external dc voltage source was applied to the NAMR, which established the coupling between the NAMR and the qubit. In a recent experiment [17], the coupling between the NAMR and the qubit can be varied between 80 MHz to 160 MHz, by adjusting the external voltage ($V_{NR} = 5 - 10V$). Thus, in our system, a strong and tunable coupling between the NAMR and the CPW microwave cavity mediated via Transmon qubit can be achieved. With this setup, the transfer of quantum information between the NAMR and CPW microwave cavity can be accomplished. On the other hand, it has been reported in many experimental studies that the mechanical gain can be achieved via directly driving the mechanical modes including Josephson Phase qubit [57], piezoelectric pump [58], microwave electrical driving [59], and by phonon lasing method [60]. Hence, by considering both the cavity gain and the mechanical loss, the transition

from the broken PT -symmetry phase to the unbroken PT -symmetry phase can be obtained in our system.

VII. ACKNOWLEDGMENT

Jameel Hussain gratefully acknowledges support from the COMSATS University Islamabad for providing him a workspace.

* Electronic address: javedakram@daad-alumni.de

- [1] M. D. Lukin, *Rev. Mod. Phys.* **75**, 457 (2003).
- [2] R. Hanson and D. D. Awschalom, *Nature (London)* **453**, 1043 (2008).
- [3] S. Ashhab, A. O. Niskanen, K. Harrabi, Y. Nakamura, T. Picot, P. C. de Groot, C. J. P. M. Harmans, J. E. Mooij, and F. Nori, *Phys. Rev. B* **77**, 014510 (2008).
- [4] G.-L. Cheng, Y.-P. Wang, W.-X. Zhong, and A.-X. Chen, *Ann. Phys.* **353**, 64 (2015).
- [5] L. Tian, *Phys. Rev. B* **72**, 195411 (2005).
- [6] G. Chen, Z. Chen, L. Yu, and J. Liang, *Phys. Rev. A* **76**, 024301 (2007).
- [7] F. Xue, Y. D. Wang, C. P. Sun, H. Okamoto, H. Yamaguchi, and K. Semba, *New J. Phys.* **9**, 35 (2007).
- [8] J. Akram and F. Saif, *J. Russ. Laser Res.* **29**, 538 (2008).
- [9] Z.-L. Xiang, S. Ashhab, J. Q. You, and F. Nori, *Rev. Mod. Phys.* **85**, 623 (2013).
- [10] F. Xue, Y.-x. Liu, C. P. Sun, and F. Nori, *Phys. Rev. B* **76**, 064305 (2007).
- [11] G. Z. Cohen and M. Di Ventra, *Phys. Rev. B* **87**, 014513 (2013).
- [12] T. L. Schmidt, K. Børkje, C. Bruder, and B. Trauzettel, *Phys. Rev. Lett.* **104**, 177205 (2010).
- [13] P. Zhang, Y. D. Wang, and C. P. Sun, *Phys. Rev. Lett.* **95**, 097204 (2005).
- [14] K. Xia and J. Evers, *Phys. Rev. Lett.* **103**, 227203 (2009).
- [15] J. Zhang, Y.-x. Liu, and F. Nori, *Phys. Rev. A* **79**, 052102 (2009).
- [16] Y.-x. Liu, A. Miranowicz, Y. B. Gao, J. c. v. Bajer, C. P. Sun, and F. Nori, *Phys. Rev. A* **82**, 032101 (2010).
- [17] J.-M. Pirkkalainen, S. Cho, F. Massel, J. Tuorila, T. Heikkilä, P. Hakonen, and M. Sillanpää, *Nat. Commun.* **6**, 6981 (2015).
- [18] J. Hussain, M. Nouman, F. Saif, and J. Akram, *Phys. B: Condens. Matter* **587**, 412152 (2020).
- [19] A. Ayoub and J. Akram, *Physica C: Superconductivity and its Applications* **591**, 1353977 (2021).
- [20] C. E. Rüter, K. G. Makris, R. El-Ganainy, D. N. Christodoulides, M. Segev, and D. Kip, *Nat. Phys.* **6**, 192 (2010).
- [21] H. Cartarius and G. Wunner, *Phys. Rev. A* **86**, 013612 (2012).
- [22] H. Jing, S. K. Özdemir, X.-Y. Lü, J. Zhang, L. Yang, and F. Nori, *Phys. Rev. Lett.* **113**, 053604 (2014).
- [23] X.-W. Xu, Y.-x. Liu, C.-P. Sun, and Y. Li, *Phys. Rev. A* **92**, 013852 (2015).
- [24] C. Hang, G. Huang, and V. V. Konotop, *Phys. Rev. Lett.* **110**, 083604 (2013).
- [25] D. Haag, D. Dast, A. Löhle, H. Cartarius, J. Main, and G. Wunner, *Phys. Rev. A* **89**, 023601 (2014).
- [26] F. Quijandría, U. Naether, S. K. Özdemir, F. Nori, and D. Zueco, *Phys. Rev. A* **97**, 053846 (2018).
- [27] J. Akram, A. Hussain, M. Nouman, and J. Hussain, *J. Opt. Soc. Am. B* **38**, 1984 (2021).
- [28] J. Hussain, J. Akram, and F. Saif, *J. Low Temp. Phys.* **195**, 429 (2019).
- [29] B. Gardas, S. Deffner, and A. Saxena, *Phys. Rev. A* **94**, 040101 (2016).
- [30] K. Kawabata, Y. Ashida, and M. Ueda, *Phys. Rev. Lett.* **119**, 190401 (2017).
- [31] S.-L. Chen, G.-Y. Chen, and Y.-N. Chen, *Phys. Rev. A* **90**, 054301 (2014).
- [32] H. Xu, L. Mason, D. and Jiang, and J. G. E. Harris, *Nature (London)* **537**, 80 (2016).
- [33] J. Doppler, A. A. Mailybaev, J. Böhm, A. Kuhl, Ulrich; Girschik, F. Libisch, T. J. Milburn, N. Rabl, Peter; Moiseyev, and S. Rotter, *Nature (London)* **547**, 76 (2016).
- [34] Z. Zhang, L. Yang, J. Feng, J. Sheng, Y. Zhang, Y. Zhang, and M. Xiao, *Laser and Photonics Rev.* , 1800155 (2018).
- [35] X. Li, D. Zhang, D. Zhang, L. Hao, H. Chen, Z. Wang, and Y. Zhang, *Phys. Rev. A* **97**, 053830 (2018).
- [36] G. S. Agarwal and K. Qu, *Phys. Rev. A* **85**, 031802 (2012).
- [37] K. V. Kepesidis, T. J. Milburn, J. Huber, K. G. Makris, S. Rotter, and P. Rabl, *New J. Phys.* **18**, 095003 (2016).
- [38] M. Zhang, W. Sweeney, C. W. Hsu, L. Yang, A. D. Stone, and L. Jiang, *Phys. Rev. Lett.* **123**, 180501 (2019).
- [39] T. Yu and J. H. Eberly, *Phys. Rev. Lett.* **93**, 140404 (2004).
- [40] J.-H. Huang and S.-Y. Zhu, *Opt. Commun.* **281**, 2156 (2008).
- [41] S. Vashahri-Ghamsari, B. He, and M. Xiao, *Phys. Rev. A* **96**, 033806 (2017).
- [42] J. Laurat, K. S. Choi, H. Deng, C. W. Chou, and H. J. Kimble, *Phys. Rev. Lett.* **99**, 180504 (2007).
- [43] M. P. Almeida, F. de Melo, M. Hor-Meyll, A. Salles, S. P. Walborn, P. H. S. Ribeiro, and L. Davidovich, *Science* **316**, 579 (2007).
- [44] J. P. Paz and A. J. Roncaglia, *Phys. Rev. Lett.* **100**, 220401 (2008).
- [45] C. Cormick and J. P. Paz, *Phys. Rev. A* **78**, 012357 (2008).
- [46] J. Koch, T. M. Yu, J. Gambetta, A. A. Houck, D. I. Schuster, J. Majer, A. Blais, M. H. Devoret, S. M. Girvin, and R. J. Schoelkopf, *Phys. Rev. A* **76**, 042319 (2007).
- [47] M. Abdi, M. Pernpeintner, R. Gross, H. Huebl, and M. J. Hartmann, *Phys. Rev. Lett.* **114**, 173602 (2015).
- [48] E. K. Irish and K. Schwab, *Phys. Rev. B* **68**, 155311 (2003).
- [49] M. Aspelmeyer, T. J. Kippenberg, and F. Marquardt, *Rev. Mod. Phys.* **86**, 1391 (2014).
- [50] H. Fröhlich, *Phys. Rev.* **79**, 845 (1950).
- [51] S. L. Braunstein and P. van Loock, *Rev. Mod. Phys.* **77**, 513 (2005).
- [52] K. Børkje, A. Nunnenkamp, and S. M. Girvin, *Phys. Rev. Lett.* **107**, 123601 (2011).
- [53] A. M. I. L. C. A. M. H. S. G. S. Riedinger, Ralf; Wallucks, *Nature* **556**, 473 (2018).
- [54] C. F. Ockeloen-Korppi, E. Damskägg, J.-M.

- Pirkkalainen, M. Asjad, A. A. Clerk, F. Massel, M. J. Woolley, and M. A. Sillanpää, *Nature (London)* **556**, 478 (2018).
- [55] I. Marinković, A. Wallucks, R. Riedinger, S. Hong, M. Aspelmeyer, and S. Gröblacher, *Phys. Rev. Lett.* **121**, 220404 (2018).
- [56] J. Naikoo, K. Thapliyal, S. Banerjee, and A. Pathak, *Phys. Rev. A* **99**, 023820 (2019).
- [57] A. D. O’Connell, M. Hofheinz, M. Ansmann, R. C. Bialczak, M. Lenander, E. Lucero, M. Neeley, D. Sank, H. Wang, and M. Weides, *Nature* **464**, 697 (2010).
- [58] C. Xiong, L. Fan, X. Sun, and H. X. Tang, *Appl. Phys. Lett.* **102**, 021110 (2013).
- [59] J. Bochmann, A. Vainsencher, D. D. Awschalom, and A. N. Cleland, *Nat. Phys.* **9**, 712 (2013).
- [60] G. Bahl, M. Tömes, F. Marquardt, and T. Carmon, *Nat. Phys.* **8**, 203 (2012).